

Non-Fermi-liquid behaviour at the pressure-induced antiferromagnetic to nonmagnetic transition in a heavy-fermion compound, CeNi_3

This article has been downloaded from IOPscience. Please scroll down to see the full text article.

1996 J. Phys.: Condens. Matter 8 9743

(<http://iopscience.iop.org/0953-8984/8/48/006>)

View [the table of contents for this issue](#), or go to the [journal homepage](#) for more

Download details:

IP Address: 171.66.16.207

The article was downloaded on 14/05/2010 at 05:41

Please note that [terms and conditions apply](#).

Non-Fermi-liquid behaviour at the pressure-induced antiferromagnetic to nonmagnetic transition in a heavy-fermion compound, Ce_7Ni_3

Kazunori Umeo[†], Hideoki Kadomatsu[‡] and Toshiro Takabatake[†]

[†] Department of Materials Science, Faculty of Science, Hiroshima University, Higashi-Hiroshima 739, Japan

[‡] Cryogenic Centre, Hiroshima University, Higashi-Hiroshima 739, Japan

Received 17 September 1996

Abstract. High-pressure studies of transport, magnetic and thermal properties of a heavy-fermion antiferromagnet, Ce_7Ni_3 , are reviewed. At ambient pressure, the Ce ions in the three nonequivalent sites in this compound are found to be very close to trivalent from L_{III} -XANES (x-ray absorption near-edge structure) spectra and magnetic susceptibility measurements. With increasing pressure, T_N (1.8 K at $P = 0$) of Ce_7Ni_3 is suppressed and vanishes near $P_c \approx 0.32$ GPa. Non-Fermi-liquid (NFL) behaviour appears around 0.4 GPa in both the specific heat and AC magnetic susceptibility: $C_m/T \propto -\ln T$ and $\chi_{AC} \propto (1 - \alpha T^{1/2})$. Above 0.62 GPa, the normal Fermi liquid state recovers as indicated by the T independence of C_m/T and the T^2 dependence of magnetic resistivity. The variation of $C_m(T)$ with pressure is analysed in terms of two models: the impurity Kondo model with three Kondo temperatures and the self-consistent renormalization (SCR) theory of spin fluctuations (SFs). We find that the crossover in C_m/T is better described by the SCR theory. The characteristic SF temperature T_0 increases by a factor of 20 for $0.33 \text{ GPa} \leq P \leq 0.75 \text{ GPa}$, yielding a large Grüneisen parameter $\Gamma_e = 220$ around 0.4 GPa.

1. Introduction

Recently, non-Fermi-liquid (NFL) behaviours in specific heat $C/T \propto -\ln T$, magnetic susceptibility $\chi \propto (1 - T^{1/2})$ and resistivity $\Delta\rho \propto T$ have been reported for some uranium- and cerium-based alloys when the magnetic state is destroyed by the substitution of the constituent elements. A two-channel Kondo model was proposed to explain the NFL behaviour in U-based systems such as $\text{U}_{0.2}\text{Y}_{0.8}\text{Pd}_3$ [1], $\text{Th}_{1-x}\text{U}_x\text{Ru}_2\text{Si}_2$ ($x \leq 0.07$) [2] and $\text{U}_{0.9}\text{Th}_{0.1}\text{Be}_{13}$ [3]. However, this model is not adequate to describe the NFL behaviour observed in $\text{CeCu}_{5.9}\text{Au}_{0.1}$ [4], $\text{CePtSi}_{0.9}\text{Ge}_{0.1}$ [5] and $\text{Ce}_{1-x}\text{La}_x\text{Ru}_2\text{Si}_2$ [6, 7] with orthorhombic or tetragonal site symmetry for Ce^{3+} . In both $\text{CeCu}_{6-x}\text{Au}_x$ and $\text{CePtSi}_{1-x}\text{Ge}_x$, the ground state changes from a nonmagnetic state to an antiferromagnetically ordered state near $x_c = 0.1$, where the NFL behaviour has been observed.

Dobrosavljević *et al* have shown that a distribution of T_K in a disordered system induces diverging magnetic susceptibility χ as $T \rightarrow 0$, i.e., NFL behaviour [8]. Bernal *et al* have shown that the temperature dependences of χ and C of $\text{UCu}_{5-x}\text{Pd}_x$ are in agreement with the model [9]. The distribution in T_K can be led from fluctuations in the exchange coupling between the 4f and conduction electrons, J , or in the density of state of conduction electrons, $N(E_F)$.

Moriya and Takimoto have applied the self-consistent renormalization (SCR) theory of spin fluctuations (SFs) to the heavy-fermion systems near the antiferromagnetic instability [10]. They have argued that the dynamical susceptibility of the systems, mainly due to the f electrons, can be described in terms of mutually interacting local SFs. According to the SCR theory, the temperature dependence of specific heat and resistivity is represented as a function of the characteristic SF energy T_0 [10]. The calculations have shown that the specific heat and resistivity exhibit temperature variations of the NFL form, $C/T \propto -\ln T$ and $\rho \propto T$ in a certain range of temperature around T_0 , which respectively change into the low-temperature forms, $C/T \propto (1 - T^{1/2})$ and $\rho \propto T^{3/2}$ at the critical boundary ($y_0 = 0$). Kambe *et al* have used this theory to analyse the data of C and ρ of $\text{Ce}_{1-x}\text{La}_x\text{Ru}_2\text{Si}_2$ [6, 7] and $\text{CeCu}_{6-x}\text{Au}_x$ [7], and have argued that the NFL behaviour is the consequence of antiferromagnetic SFs of 4f electrons with characteristic energy much smaller than that in itinerant 3d-electron systems. They have pointed out further that the lattice disorder introduced by the alloying must be taken into account, because the SCR theory assumes a perfect lattice. Therefore, a systematic study of physical properties near the magnetic instability is highly desired on a heavy-fermion compound with an ordered crystal structure. In this respect, we should recall that for magnetically ordered Ce compounds pressure increases hybridization and the magnetic order becomes unstable [11]. Indeed, a pressure-induced transition from the antiferromagnetic to the nonmagnetic state has been found in several compounds, e.g., CeIn_3 [12], CeRh_2Si_2 [13] and CeCu_2Ge_2 [14]. For the antiferromagnetic heavy-fermion alloy $\text{CeCu}_{5.7}\text{Au}_{0.3}$ ($T_N = 0.49$ K for $P = 0$), the NFL behaviour in $C(T)$ was observed at the critical pressure $P_c = 0.82$ GPa where T_N vanishes [15]. More recently, pressure-induced NFL behaviour has been observed in $\rho(T)$ of CePd_2Si_2 [16] and in $C(T)$ of CeCu_2Si_2 [17] near the antiferromagnetic to superconducting transition.

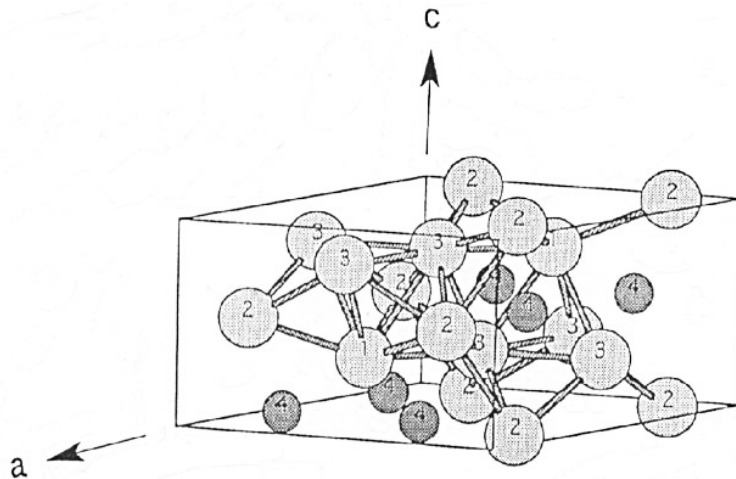


Figure 1. The hexagonal Th_7Fe_3 -type structure for Ce_7Ni_3 . The atoms 1–4 are Ce_I , Ce_{II} , Ce_{III} and Ni, respectively.

In the Ce–Ni binary phase diagram there exist six ordered compounds, which show various magnetic and electronic properties. The cerium in CeNi_5 and CeNi possesses the intermediate valence state [18], leading to a nonmagnetic ground state. On the other hand, Ce_7Ni_3 orders antiferromagnetically below 1.8 K [18]. Sereni *et al* have found that the

magnetic order coexists with a heavy-fermion state ($\gamma = 9 \text{ J K}^{-2} \text{ mol}^{-1} \text{ f.u.}$) [19]. Ce_7Ni_3 crystallizes in the hexagonal Th_7Fe_3 -type structure (space group $P6_3mc$) as shown in figure 1 [20]. There are three nonequivalent crystallographic Ce sites (I, II and III). The site I (one Ce atom) has trigonal symmetry (point group C_{3v}), and both site II (three Ce atoms) and III (three Ce atoms) have monoclinic symmetry (point group C_{1v}). Sites I and II have enough space for Ce^{3+} ions, while the space of the site III is about 5% smaller and the trivalent state might be unstable [19]. From the comparison of the specific heat of Ce_7Ni_3 with that of Ce_7Rh_3 , it was conjectured that the Ce_I in Ce_7Ni_3 antiferromagnetically orders, the Ce_{II} behaves as Kondo impurities with $T_K \approx 4 \text{ K}$ and the Ce_{III} is in the intermediate valence state with a characteristic temperature $T_0 \approx 70 \text{ K}$ [19]. However, from Ce 3d x-ray photoelectron spectroscopy (XPS) [21] and bremsstrahlung isochromat spectroscopy (BIS) [22], the relative intensities of the 'f⁰' peaks in spectra were estimated to be less than 0.05 and 0.02–0.08, respectively. These results suggest that the valence of all the Ce ions in Ce_7Ni_3 is very close to three. In order to check the above argument, we have measured Ce L_{III} XANES (x-ray absorption near-edge structure) spectra and magnetic susceptibility.

Since the T_N ($=1.8 \text{ K}$) for Ce_7Ni_3 is rather low, it is expected that the antiferromagnetism can be destroyed by the application of pressure in our accessible range. Near the transition from magnetic to nonmagnetic state, we anticipate the appearance of NFL behaviour. As a matter of fact, we have found in Ce_7Ni_3 the pressure-induced transition by measurements of specific heat, AC magnetic susceptibility and electrical resistivity. In this paper, we present such results and discuss them in terms of the SCR theory of SFs.

2. Results

2.1. Valence states of Ce_7Ni_3 at ambient pressure

The L_{III} -XANES has been used widely to assess the valence of Ce in many heavy-fermion and intermediate-valence compounds [23]. There will be two absorption peaks corresponding to trivalent and tetravalent states in the L_{III} spectra, and the relative intensities give a determination of the valence. In fact, for intermediate-valence compounds such as $CeNi_2$, $CeNi_5$ and $CePd_3$, two white lines separated by 9 eV have been observed [23].

Figure 2 shows Ce L_{III} XANES spectra for Ce_7Ni_3 at 300 and 10 K, after the background has been subtracted. The two spectra are identical and exhibit a single peak of the L_{III} edge at 5720 eV. The absence of the tetravalent peak suggests that the valence of all the Ce ions in Ce_7Ni_3 is close to three over the entire temperature range.

The magnetic susceptibility and its inverse along the three principal axes of Ce_7Ni_3 are presented in figure 3, where the b axis is defined perpendicular to the a axis. The anisotropy between the c axis and the a – b plane is significant but the anisotropy between the a and b axes is very weak. Above 100 K, the data follow a Curie–Weiss law with paramagnetic Curie temperatures of -67 and -24 K for $H \perp c$ and $H \parallel c$, respectively. The effective magnetic moments per Ce atom are respectively 2.61 and $2.52 \mu_B$, which are very close to the free Ce^{3+} ion value ($2.54 \mu_B$). This fact is a further indication of the trivalent valences for Ce ions in the three (I, II and III) sites. Therefore, the electronic states of Ce ions in the III site may not be distinguishable from those in the I and II sites. The deviation of the susceptibility data from the Curie–Weiss law, which becomes noticeable below 50 K, may arise from the crystalline electric field effect.

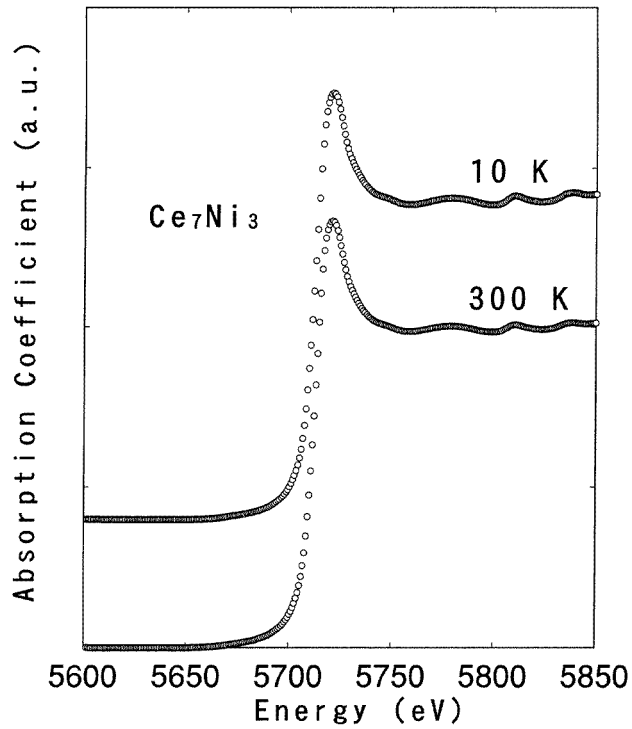


Figure 2. Ce L_{III} XANES spectra of Ce_7Ni_3 at 300 and 10 K.

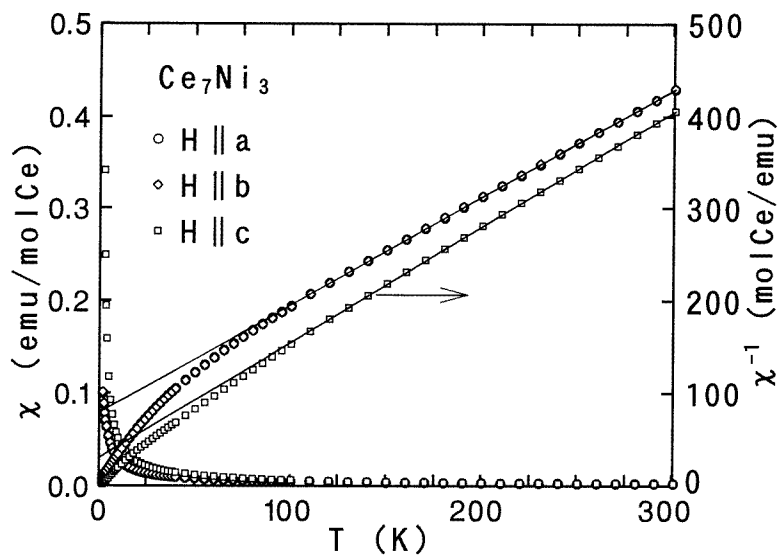


Figure 3. DC magnetic susceptibility and the inverse along the a , b , and c axes of a Ce_7Ni_3 single crystal, where the b axis is defined as perpendicular to the a axis.

2.2. Physical properties of Ce_7Ni_3 at high pressures

The methods of sample preparation and measurement have been described in [24,25]. Figure 4 shows the temperature dependence of the AC magnetic susceptibility $\chi_{AC}(T)$

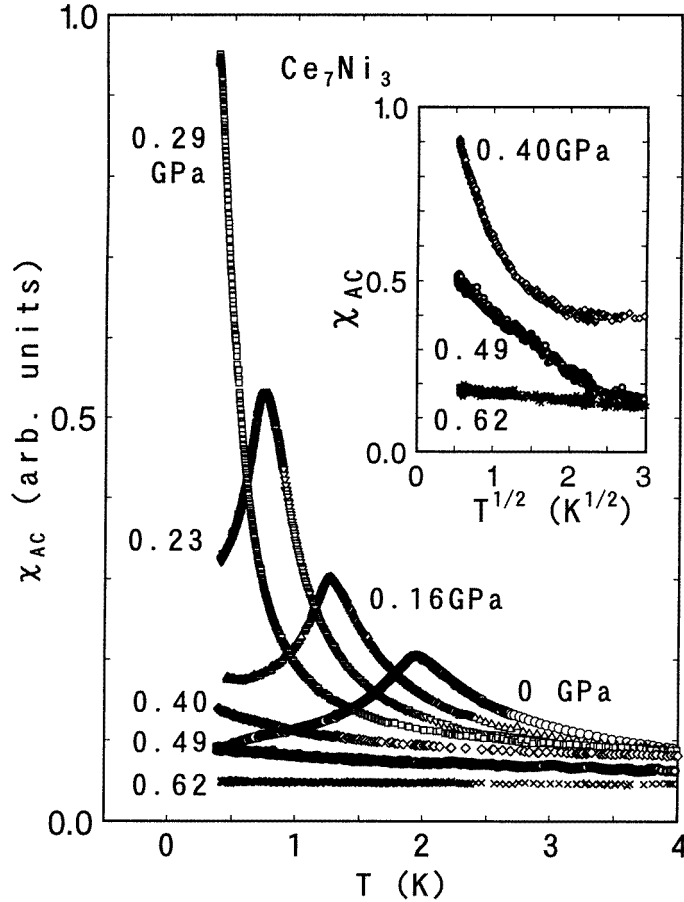


Figure 4. Temperature dependence of AC magnetic susceptibility χ_{AC} of polycrystalline Ce_7Ni_3 at various pressures. The inset shows $\chi_{AC}(T)$ against $T^{1/2}$ above 0.40 GPa.

of a polycrystalline sample of Ce_7Ni_3 at various pressures up to 0.62 GPa. At ambient pressure, the maximum at 1.9 K indicates the onset of the antiferromagnetic order. A broad swell exists around 0.6 K, where a weak anomaly in specific heat has been reported [19]. With increasing pressure up to 0.29 GPa, T_N defined by the maximum temperature in $\chi_{AC}(T)$ decreases and the value of χ_{AC} at T_N strongly increases. Above 0.4 GPa, χ_{AC} is greatly reduced over the measured temperature range. In order to trace the transition from the NFL behaviour to Fermi liquid behaviour, we present in the inset of figure 4 the data of χ_{AC} against $T^{1/2}$ at selected pressures between 0.40 and 0.62 GPa. At 0.40 GPa, the NFL behaviour, $\chi_{AC} \propto (1 - \alpha T^{1/2})$, is observed only below 1 K, while at 0.49 GPa it is observed up to 5 K. At 0.62 GPa, χ_{AC} becomes almost independent of temperature, indicating the recovery of the Fermi liquid state.

Figure 5 shows $C(T)$ of Ce_7Ni_3 and La_7Ni_3 at various pressures. For $P = 0$, a λ -type anomaly appears at $T_N = 1.8$ K. With increasing pressure, both the specific heat jump $\Delta C(T_N)$ and T_N decrease and vanish above 0.33 GPa. The $C(T)$ at low temperatures decreases steeply with pressure, while that of La_7Ni_3 hardly changes. The magnetic

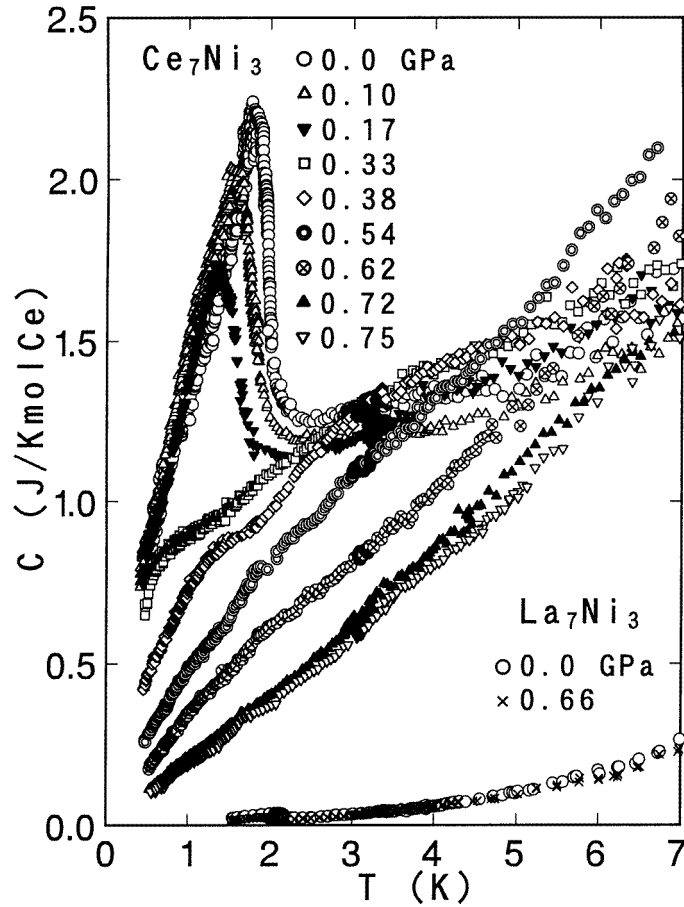


Figure 5. The temperature dependence of the specific heat of Ce_7Ni_3 and La_7Ni_3 at various pressures.

contribution to the specific heat C_m was estimated by the subtraction of C for La_7Ni_3 . For this purpose, the values of C for La_7Ni_3 under pressure were estimated by linear interpolation between the two values at 0 and 0.69 GPa. The thus obtained C_m/T is plotted against $\log T$ in figure 6. At 0.33 GPa, the C_m/T curve shows an upturn. At 0.38 GPa, however, C_m/T is proportional to $-\log T$ over more than one decade in T , which is the NFL behaviour. At a higher pressure, 0.54 GPa, C_m/T has a downward curvature below 4 K. Above 0.62 GPa, C_m/T is saturated at low temperatures, indicating the recovery of the normal Fermi liquid state. The pressure variation of $\chi_{AC}(T)$ and $C(T)$ indicates that the crossover from NFL behaviour to normal Fermi liquid behaviour takes place between 0.38 and 0.62 GPa.

Figure 7 shows the temperature dependence of electrical resistivity $\rho(T)$ along the c axis of Ce_7Ni_3 at various pressures up to 1.48 GPa together with that for La_7Ni_3 polycrystal. $\rho(T)$ at $P = 0$ has a minimum at around 40 K and two maxima at around 8 and 0.5 K, and remains at $140 \mu\Omega \text{ cm}$ at 0.4 K. The maximum at 8 K is considered to be the onset of coherent scattering of conduction electrons from periodically arrayed Ce ions. It is noteworthy that $\rho(T)$ turns up below T_N whereas magnetic scattering usually decreases

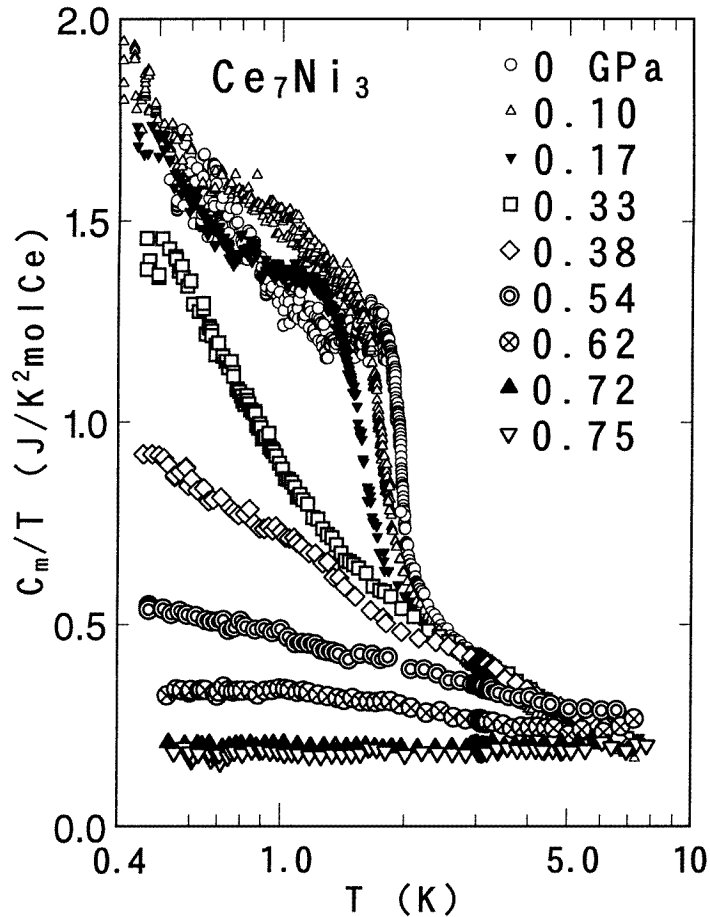


Figure 6. Magnetic contribution to the specific heat C_m/T against $\log T$ at various pressures.

below T_N . This fact suggests that the antiferromagnetic order creates a partial gap along the c axis on the Fermi surface. The lower maximum at 0.5 K may be related to some magnetic transition suggested by the anomaly in both χ_{AC} and C at 0.6 K. On applying pressure, $\rho(T)$ strongly decreases over the temperature range, and eventually $\rho(T)$ approaches that of La_7Ni_3 . The $\rho(T)$ of La_7Ni_3 decreases steeply with decreasing temperature, and exhibits a superconducting transition at 2.1 K.

The magnetic contribution to $\rho(T)$ from 4f electrons was estimated by using the relation of $\rho_m(P, T) = \rho(Ce_7Ni_3) - \rho(La_7Ni_3)$. Double-logarithmic plot of $\rho_m(T) - \rho_m(0)$ against T above 0.66 GPa are presented in figure 8. We find the relation $\rho_m(T) - \rho_m(0) = AT^2$, which is characteristic of a Fermi liquid, as indicated by the straight lines. As pressure increases, the temperature range in which the above relation holds becomes wider and the coefficient A decreases dramatically, as shown in the inset of figure 8.

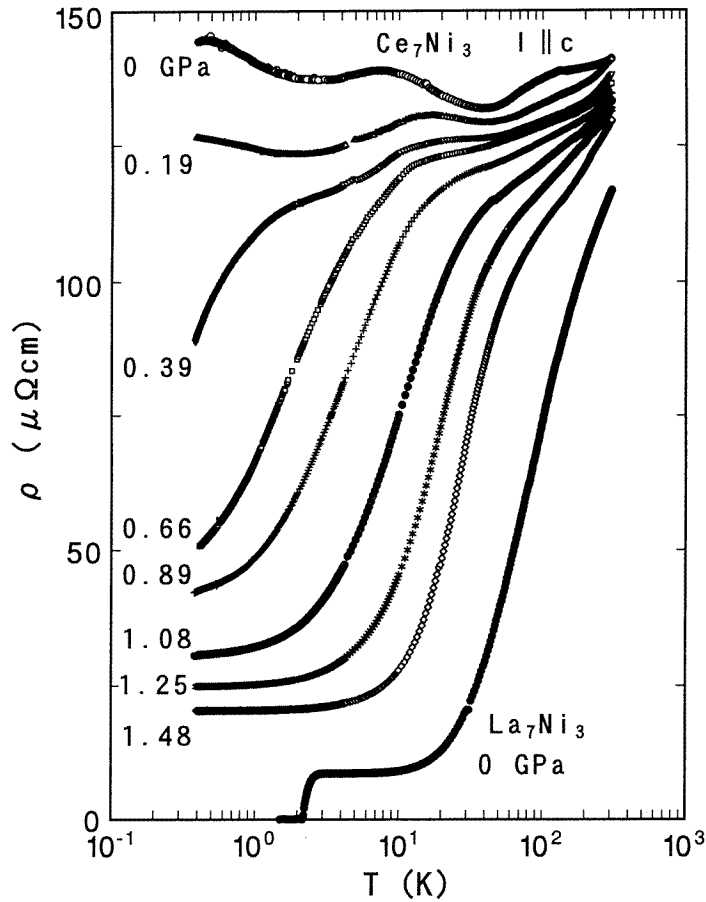


Figure 7. The temperature dependence of the electrical resistivity along the c axis of a Ce_7Ni_3 single crystal at various pressures up to 1.48 GPa.

3. Discussion

3.1. Pressure dependence of T_N

The pressure dependence of T_N for Ce_7Ni_3 determined from $\chi_{AC}(T)$ and $C(T)$ is shown in figure 9. Assuming the form $T_N \propto |P - P_c|^n$, the parameters P_c and n are estimated to be 0.32 GPa and 0.63, respectively. The solid line in the figure is the fitting result. The exponent n is close to two-thirds, which value was predicted for an antiferromagnet in three spatial dimensions by Millis using renormalization-group techniques [26]. By using the bulk modulus $B_0 = 24.6$ GPa [24], the Grüneisen parameter $\Gamma_N = -B_0 \ln T_N / \partial \ln P = \ln T_N / \partial \ln V$ at $P = 0$ is found to be 74. This value is much greater than that of Ce compounds with similar values of T_N such as CeAl_2 ($T_N = 3.8$ K, $\Gamma_N = 12$) [12]. The Γ_N for Ce_7Ni_3 becomes approximately 3000 around 0.3 GPa. The large Grüneisen parameter may be the combined effects of the electronic state being close to the magnetic–nonmagnetic transition and of the critical balance between the Kondo and RKKY interaction at ambient pressure.

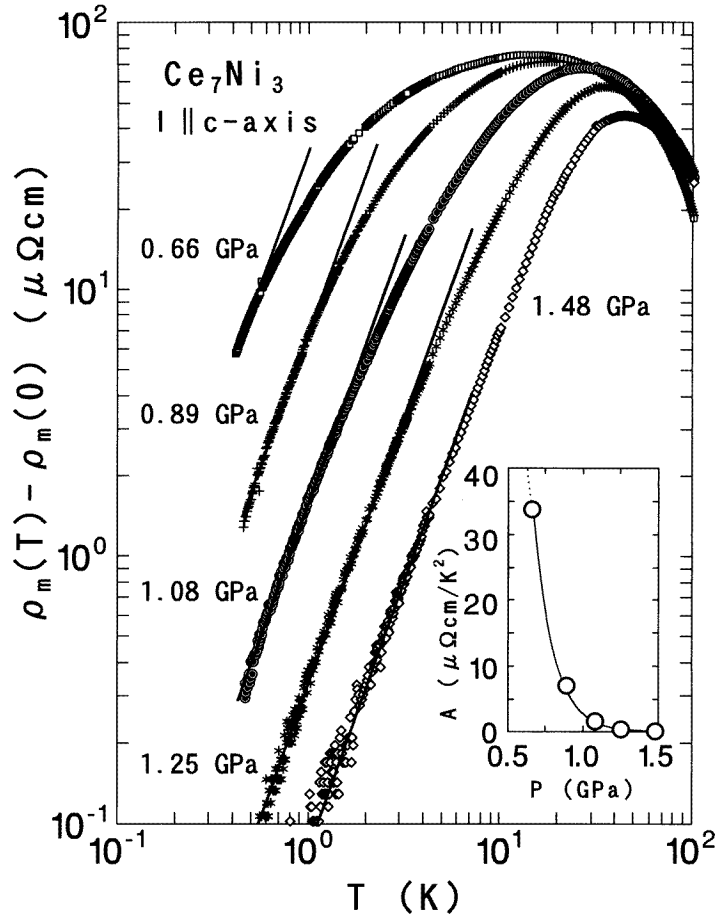


Figure 8. Double-logarithmic plots of the magnetic contribution to electrical resistivity $\rho_m(T) - \rho_m(0)$ against T for Ce_7Ni_3 at various pressures. Solid lines represent the form $\rho_m(T) - \rho_m(0) = AT^2$. The pressure dependence of A is shown in the inset.

3.2. The crossover from non-Fermi liquid to Fermi liquid

We now discuss the crossover from NFL behaviour to Fermi liquid behaviour for Ce_7Ni_3 observed above $P_c = 0.32$ GPa. Different scenarios for the origin of NFL behaviour have been proposed so far: (i) the two-channel Kondo effect [27]; (ii) the impurity Kondo model with distributed Kondo temperatures [8,9] and (iii) the self-consistent renormalized (SCR) theory of SFs [10]. The applicabilities of the first two models are briefly discussed.

The two-channel magnetic Kondo effect may occur in cerium compounds with Ce^{3+} ions in cubic and hexagonal symmetry sites [27]. Among the three nonequivalent Ce sites in Ce_7Ni_3 , the site I for one Ce atom has trigonal symmetry, and the sites II and III with three Ce atoms each have monoclinic symmetry. Therefore, the two-channel Kondo effect is unlikely to occur in this compound.

Next, we will discuss the applicability of the impurity Kondo model with distributed Kondo temperatures. Because there are nonequivalent sites for Ce atoms in Ce_7Ni_3 , the exchange coupling between the 4f and conduction electrons J may distribute so that the

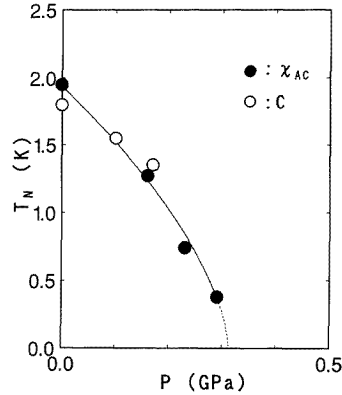


Figure 9. Pressure dependence of T_N determined by AC magnetic susceptibility (●) and specific heat (○) measurements. The solid line shows the fitting curve of the form $T_N = C|P - P_c|^n$.

T_K may be different for the three sites. In general, T_K may depend on the site symmetry and inter-atomic spaces of Ce ions. Considering the Ce and Ni atoms as rigid spheres, atomic radii of Ce_I , Ce_{II} and Ce_{III} are estimated to be 1.81, 1.76 and 1.72 Å, respectively [18]. Therefore, we assume that the three Kondo temperatures are in order of the inverse of the volume, $T_{K1}(Ce_I) < T_{K2}(Ce_{II}) < T_{K3}(Ce_{III})$. We further assume that the magnetic specific heat C_m is described by the summation of independent contributions from three types of Kondo impurity with spin 1/2 [28], $C_m/T = C_{K1}(I) + C_{K2}(II) + C_{K3}(III)$. The fitted results of $C_{K1} + C_{K2} + C_{K3}$ for 0.38 and 0.54 GPa are shown by dotted lines in figure 10(a) and (b), respectively. T_{K1} , T_{K2} and T_{K3} are respectively 2, 10 and 24 K at 0.38 GPa, and 5.5, 19 and 30 K at 0.54 GPa. For comparison, the results of SCR theory (C_{SCR}) are shown as the solid lines. We will see that the SCR theory with fewer fitting parameters reproduces better the experimental data than the impurity Kondo model.

We now apply the SCR theory to describe the observed $C_m(T)$, $\chi_{AC}(T)$ and $\rho_m(T)$ of Ce_7Ni_3 . The theory involves three important parameters y_0 , χ_c and T_0 , which represent respectively the reduced inverse staggered susceptibility at 0 K, the cut-off wave vector in units of q_B and the characteristic SF energy in the energy space (see [10] for these notations). Assuming that the electronic states of Ce ions are identical for the three sites, we will discuss the pressure dependence of $C_m(T)$ for $P \geq 0.33$ GPa. The solid lines in figure 11 are the fits using the calculated results in figure 1(b) of [10], assuming $y_0 = 0$ for $0.33 \text{ GPa} \leq P \leq 0.54 \text{ GPa}$, $y_0 = 0.02$ for $P = 0.62 \text{ GPa}$ and $y_0 = 0.1$ for $P \geq 0.72 \text{ GPa}$. The parameters y_0 , χ_c and T_0 are listed in table 1. At the critical boundary, C_m/T is expected to follow the form $C_m/T = \gamma_0 - \beta T^{1/2}$ for $T \ll T_0$. This form is not observed at $P = 0.33$ and 0.38 GPa down to 0.5 K because this temperature is not sufficiently below T_0 . At $P = 0.54$ GPa, however, C_m/T follows the above form between 0.5 and 3 K, being far below $T_0 = 13.5$ K. The NFL behaviour appears in the range of small characteristic SF energy.

It is noteworthy that in figure 4 the value of χ_{AC} at 0.6 K is reduced by one order of magnitude once the antiferromagnetic state disappears. The static uniform susceptibility χ_n at $T \approx 0$ K can be expressed as $\chi_n = 1/(2(1 + y_0)T_A)$, where T_A is the characteristic SF energy in the momentum space [10]. The observed decrease of χ_{AC} implies the increase of y_0 and/or T_A with increasing pressure. The relation of $J_Q/T_A = 1$ [10] in turn suggests

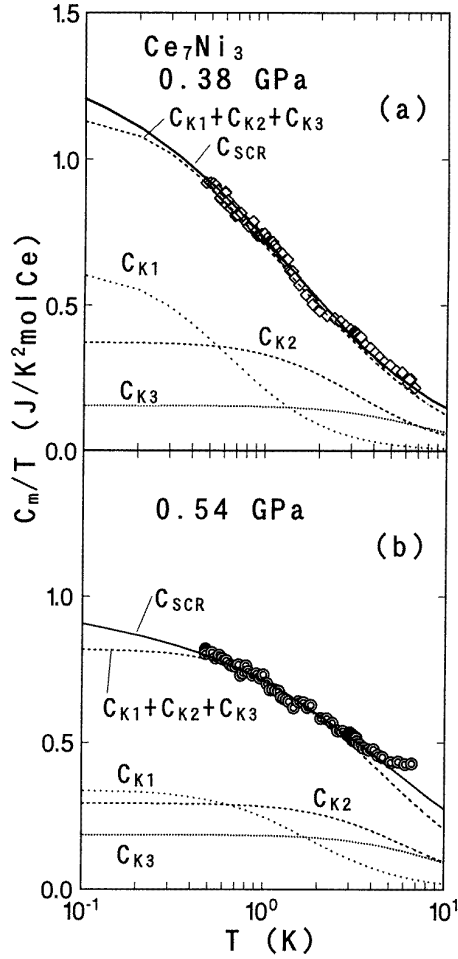


Figure 10. Fitting results of the magnetic specific heat C_m/T at 0.38 GPa (a) and 0.54 GPa (b) by the impurity Kondo model, with three Kondo temperatures for the three Ce sites. The solid lines, C_{SCR} , represent the fits by the SCR theory.

Table 1. Characteristic parameters of SCR theory for Ce_7Ni_3 obtained by fitting the temperature dependence of C_m/T under pressure. Parameters y_0 , χ_c and T_0 are the reduced inverse staggered susceptibility at 0 K, the cut-off wave vector in units of q_B and the characteristic SF energy in the energy space, respectively [10].

P (GPa)	y_0	χ_c	T_0 (K)
0.33	0	0.57	2.3
0.38	0	0.60	5.2
0.54	0	0.71	13.5
0.62	0.02	0.75	21.5
0.72	0.1	1.0	37
0.75	0.1	1.0	42

that pressure increases the RKKY interaction energy J_Q .

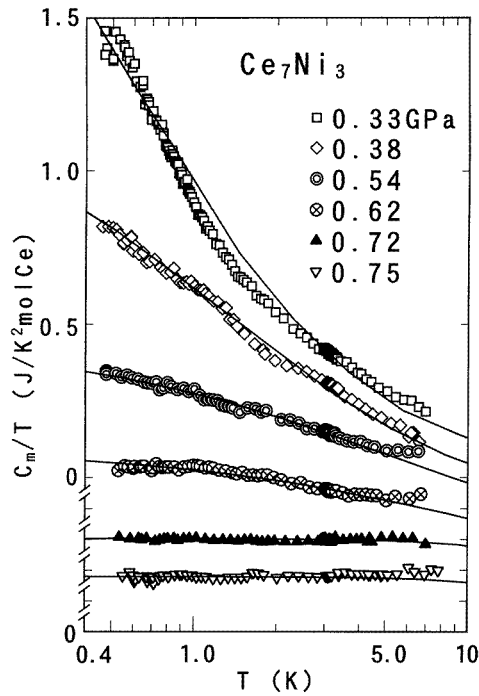


Figure 11. Magnetic specific heat divided by temperature C_m/T against $\log T$ above 0.33 GPa. Solid lines indicate the fit by the SCR theory (see the text). Data at each P are shifted downward consecutively by $0.1 \text{ J K}^{-2}/\text{mol Ce}$ for clarity.

The SCR theory leads to a relation $\rho(T) \propto (T/T_0)^{3/2}$ for $T \ll T_0$ near the critical pressure. However, at $P = 0.39 \text{ GPa}$, $\rho_m(T)$ in the low- T range cannot be described by the power law, probably because our temperature range is not sufficiently low compared to $T_0 = 5.2 \text{ K}$. For $P \geq 0.66 \text{ GPa}$, from figure 8, we find the relation $\rho_m(T) - \rho_m(0) = AT^2$. Apart from the critical boundary ($y_0 > 0$), $\rho(T)$ is expressed as

$$\rho = r(\pi/8y_0^{0.5})(T/T_0)^2 = AT^2 \quad (1)$$

where r is an adjustable parameter [10]. As shown in the inset of figure 8, the value A seems to diverge below 0.66 GPa, which tendency is expected from (1) when the critical boundary is approached. This fact supports the assumption of $y_0 = 0$ below 0.54 GPa for our analysis of the specific heat. Furthermore, the extremely strong depression of A for $P \geq 0.66 \text{ GPa}$ indicates strong increase of y_0 and/or T_0 , which is consistent with the result of $T_0(P)$ deduced from that of the specific heat.

3.3. The pressure dependence of the Kondo effect and spin fluctuations

In this section, we discuss the specific heat and electrical resistivity in the normal Fermi liquid region above 0.62 GPa. In the Fermi liquid state, the Sommerfeld coefficient, γ , and the coefficient A of the T^2 dependence of electrical resistivity are related by $\gamma^2 \propto A$. For many Ce- and U-based compounds, A/γ^2 has a universal value of $1.0 \times 10^{-5} (\mu\Omega \text{ cm/K}^{-2})/(\text{mJ mol}^{-1} \text{ K}^{-2})$ [29]. The values of A at 0.62 and 0.75 GPa for Ce_7Ni_3 were estimated by the interpolation of the results of the inset of figure 8. In figure 12, A and γ

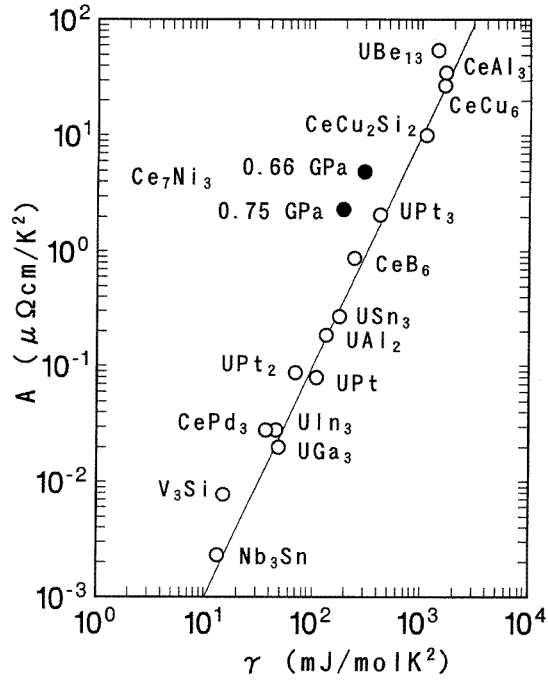


Figure 12. Coefficient A of the T^2 term of the resistivity against the coefficient γ of the T -linear term of the specific heat for various compounds. The solid line represents the ratio of $A/\gamma = 1.0 \times 10^{-5} (\mu\Omega \text{ cm/K}^2)/(\text{mJ mol}^{-1}\text{K}^{-2})$ [29].

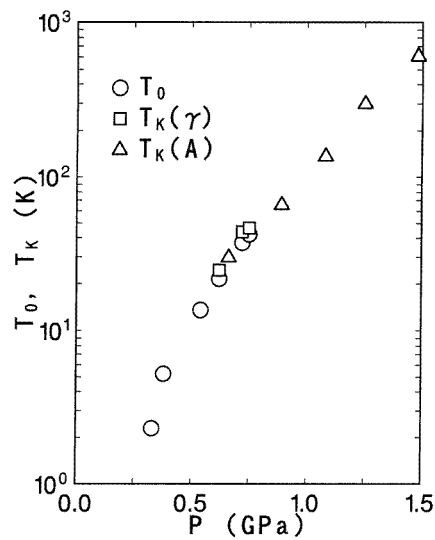


Figure 13. The pressure dependence of the SF temperature T_0 and Kondo temperature T_K .

for Ce_7Ni_3 are plotted for the data of some Ce- and U-based compounds. The values A/γ^2 at 0.62 and 0.75 GPa are 5.5×10^{-5} and $6.5 \times 10^{-5} (\mu\Omega \text{ cm/K}^{-2} \text{ mol}^{-1})/(\text{mJ mol}^{-1} \text{ K}^{-2})$,

respectively. These values are independent of pressure, which implies that the one characteristic energy scale (T_K) governs $\rho(T)$ and $C(T)$ in the normal Fermi liquid region. By the $S = 1/2$ impurity Kondo model [28], T_K is related to γ by $T_K = R\pi/(3\gamma)$, where R is the gas constant. Furthermore, the T_K above 0.75 GPa can be estimated by using the above-mentioned relation $A/\gamma^2 = 5.5 \times 10^{-5} (\mu\Omega \text{ cm}/\text{K}^{-2} \text{ mol}^{-1})/(\text{mJ mol}^{-1} \text{ K}^{-2})$. Values of T_K thus obtained agree with those of T_0 as shown in figure 13. The variation of $T_0(P)$ through the crossover continuously joins with that of $T_K(P)$ in the Fermi liquid region. It is noteworthy that the T_K representing the energy scale of the single-site SF [30], agrees with the T_0 related to the energy of the inter-site SF defined around the antiferromagnetic wave vector or antiferromagnetic correlation. This fact may imply that the antiferromagnetic correlation disappears above 0.7 GPa. The Grüneisen parameter $\Gamma_e = -\partial \ln T_0/\partial \ln V$ is estimated to be 220 around 0.4 GPa. By contrast, in $\text{Ce}_{1-x}\text{La}_x\text{Ru}_2\text{Si}_2$ and $\text{CeCu}_{6-x}\text{Au}_x$, T_0 hardly changes near the critical boundary when the unit-cell volume is decreased by decreasing x [31, 32]. The value of Γ_e for Ce_7Ni_3 decreases with increasing pressure and becomes 110 around 0.7 GPa.

4. Conclusion

We have investigated the pressure dependence of transport, magnetic and thermal properties of the heavy-fermion antiferromagnet Ce_7Ni_3 ($T_N = 1.8$ K, $\gamma = 9$ J K⁻² mol⁻¹ f.u.) possessing three nonequivalent Ce sites. When the antiferromagnetism vanishes for $P \geq 0.33$ GPa, this chemically ordered compound exhibits NFL behaviour in the AC magnetic susceptibility and specific heat. The results are summarized as follows:

(i) The L_{III} XANES and magnetic susceptibility measurements indicate that all the Ce ions in the three nonequivalent sites of Ce_7Ni_3 are trivalent at ambient pressure. This disagrees with the previous conjecture assuming an intermediate valence state for the Ce_{III} site [19].

(ii) The T_N decreases with increasing pressure as $T_N(P) \propto (P - P_c)^n$ with $P_c = 0.32$ GPa and $n = 0.63$. This critical pressure P_c is much smaller than that of usual Ce antiferromagnets with a similar value of T_N at ambient pressure, such as CeAl_2 and CeCu_2Ge_2 . The Grüneisen parameter of T_N , $\Gamma_N = \partial \ln T_N/\partial \ln V$ is also greater than that of the compounds mentioned above.

(iii) At pressures 0.33–0.49 GPa just above P_c , NFL behaviours appear in both C_m and χ_{AC} ; $C_m/T \propto -\log T$ and $\chi_{AC} \propto (1 - \alpha T^{1/2})$. For $P > 0.62$ GPa, the normal Fermi liquid behaviour is recovered, as indicated by $\rho(T) = \rho_0 + AT^2$ and the T independence of both χ_{AC} and C_m/T at low temperatures.

(iv) The crossover from the NFL behaviour to Fermi liquid behaviour in $C_m(T)$ is describable by the SCR theory of SF. The characteristic SF temperature T_0 increases by a factor of 20 for $0.32 \text{ GPa} \leq P \leq 0.75 \text{ GPa}$, yielding a large Grüneisen parameter $\Gamma_e = 220$.

(v) The coefficients A and γ decrease strongly with increasing pressure above 0.62 GPa. The continuous increase in $T_0(P)$ through the crossover ($0.33 \text{ GPa} \leq P \leq 0.75 \text{ GPa}$) joins with that of $T_K(P)$ in the Fermi liquid region ($0.66 \text{ GPa} \leq P \leq 1.48 \text{ GPa}$).

Acknowledgments

The authors would like to thank T Moriya for valuable discussions on SCR theory and NFL behaviour. We acknowledge K Izawa, T Suzuki, and T Fujita, Department of Physics, Hiroshima University, for their help in the measurement of the specific heat of Ce_7Ni_3 and

La_7Ni_3 at ambient pressure. Part of this work was done using the Heliox 3He cryostat at the Cryogenic Centre of Hiroshima University.

References

- [1] Seaman C L, Maple M B, Lee B W, Ghamaty S, Torikachvili M S, Kang J-S, Liu L Z, Allen J W and Cox D L 1991 *Phys. Rev. Lett.* **67** 2882
- [2] Amitsuka H, Hidano T, Honma T, Mitamura H and Sakakibara T 1993 *Physica B* **186-188** 337
- [3] Aliev F G, Mfarrej H El, Vieira S and Villar R 1994 *SSC* bf 91 775
- [4] v Löhneysen H, Pietrus T, Portisch G, Schlager H G, Schr der A, Sieck M and Trappmann T 1994 *Phys. Rev. Lett.* **72** 3262
- [5] Steglich F, Geibel C, Gloos K, Olesch G, Schank C, Wassilew C, Loidl A, Krimmel A and Stewart G R 1994 *J. Low-Temp. Phys.* **95** 3
- [6] Kambe S, Raymond S, Suderow H, McDonough J, Fak B, Regnault L P and Flouquet J 1996 *Physica B* at press
- [7] Kambe S, Raymond S, McDonough J, Regnault L P, Flouquet J, Lejay P and Haen P 1996 *J. Phys. Soc. Japan* at press
- [8] Dobrosavljević V, Kirkpatrick T R and Kotliar G 1992 *Phys. Rev. Lett.* **69** 1113
- [9] Bernal O O, MacLaughlin D E, Lukefahr H G and Andraka B 1995 *Phys. Rev. Lett.* **75** 2023
- [10] Moriya T and Takimoto T 1995 *J. Phys. Soc. Japan* **64** 960
- [11] Lavagna M, Lacroix C and Cyrot M 1982 *Phys. Lett.* **90A** 210
- [12] Morin P, Vettier C, Flouquet J, Konczykowski M, Lassailly Y, Mignot J-M and Welp U 1988 *J. Low Temp. Phys.* **70** 377
- [13] Thompson J D, Parks R D and Borges H 1986 *J. Magn. Magn. Mater.* **54-57** 377
- [14] Jaccard D, Behnia K and Sierro J 1992 *Phys. Lett.* **163A** 475
- [15] Bogenberger B and v Löhneysen H 1995 *Phys. Rev. Lett.* **74** 1016
- [16] Grosche F M, Julian S R, Mathur N D, McMullin G J, Pfeleiderer C and Lonzarich G G 1996 *Physica B* **223-224** 50
- [17] Steglich F, Gegenwart P, Geibel C, Helfrich R, Hellmann P, Lang M, Link A, Modler R, Sparn G, Büttgen N, Loidl A 1996 *Physica B* **223-224** 1
- [18] Gignoux D and Gomez-Sal J C 1985 *J. Appl. Phys.* **57** 3125
- [19] Sereni J G, Trovarelli O, Kappler J P, Paschke C, Trappmann T and v Löhneysen H 1994 *Physica B* **199-200** 567
- [20] Roof R B Jr, Larson A C and Cromer D T 1961 *Acta Crystallogr.* **14** 1084
- [21] Fuggle J C, Hillebrecht F U, Zolnierok Z, Lasser R, Freiburg Ch, Gunnarsson O and Schönhammer K 1983 *Phys. Rev. B* **27** 7330
- [22] Hillebrecht F U, Fuggle J C, Sawatzky G A, Campagna M, Gunnarsson O and Schönhammer K 1983 *Phys. Rev. B* **30** 1777
- [23] Wohlleben D and Röhler J 1984 *J. Appl. Phys.* **55** 1904
- [24] Umeo K, Kadomatsu H and Takabatake T 1996 *Phys. Rev. B* **54** 1194
- [25] Umeo K, Kadomatsu H and Takabatake T *Phys. Rev. B* submitted
- [26] Millis A J 1993 *Phys. Rev. B* **48** 7183
- [27] Cox D L 1993 *Physica B* **186-188** 312
- [28] Desgranges H U and Schotte K D 1982 *Phys. Lett.* **91A** 240
- [29] Kadowaki K and Woods S B 1986 *Solid State Commun.* **58** 507
- [30] Rossat-Mignod J, Regnault L P, Jacoud J L, Vettier C, Lejay P, Flouquet J, Walker E, Jaccard D and Amato A 1988 *J. Magn. Magn. Mater.* **76 & 77** 376
- [31] Quezel S, Burllet P, Jacoud J L, Regnault L P, Rossat-Mignod J, Vettier C, Lejay P and Flouquet J 1988 *J. Magn. Magn. Mater.* **76 & 77** 403
- [32] Pietrus T, Bogenberger B, Mock S, Sieck M and v Löhneysen H 1995 *Physica B* **206 & 207** 317